JOURNAL OF Applied Polymer SCIENCE

# Multifunctional Polyimide/Graphene Oxide Composites via *In Situ* Polymerization

**Jiadeng Zhu,[1,2] Jun Lim,[1] Cheol-Ho Lee,[1,2] Han-Ik Joh,[1] Hwan Chul Kim,[2] Byoungnam Park,[3] Nam-Ho You,[1] Sungho Lee[1]**

[1]Carbon Convergence Materials Research Center, Institute of Advanced Composites Materials, Korea Institute of Science and Technology, Eunha-ri san 101, Bondong-eup, Wanju-gun Jeollabuk-do, 565-905, Korea

[2]Department of Organic Materials and Fiber Engineering, Chonbuk National University, Duckjin-dong 1 Ga, Jeonju Jeollabuk-do, 561-756, Korea

[3]Department of Materials Science and Engineering, Hongik University 72-1, Sangsu-dong Mapo-gu, 121-791, Korea

Correspondence to: S. Lee (E-mail: sunghol@kist.re.kr) and N.-H. You (E-mail: polymer@kist.re.kr).

**ABSTRACT:** In this article, we detail an effective way to improve electrical, thermal, and gas barrier properties using a simple processing method for polymer composites. Graphene oxide (GO) prepared with graphite using a modified Hummers method was used as a nanofiller for r-GO/PI composites by in situ polymerization. PI composites with different loadings of GO were prepared by the thermal imidization of polyamic acid (PAA)/GO. This method greatly improved the electrical properties of the r-GO/PI composites compared with pure PI due to the electrical percolation networks of reduced graphene oxide within the films. The conductivity of r-GO/PI composites (30:70 w/w) equaled $1.1 \times 10^{1}$ S $m^{-1}$, roughly $10^{14}$ times that of pure PI and the oxygen transmission rate (OTR, 30:70 w/w) was reduced by about 93%. The Young's modulus of the r-GO/PI composite film containing 30 wt % GO increased to 4.2 GPa, which was an approximate improvement of 282% compared with pure PI film. The corresponding strength and the elongation at break decreased to 70.0 MPa and 2.2%, respectively. © 2013 Wiley Periodicals, Inc. J. Appl. Polym. Sci. **2014**, *131*, 40177.

**KEYWORDS:** composites; films; electrical conductivity; graphene oxide; gas barrier

Received 7 June 2013; accepted 7 November 2013

**DOI: 10.1002/app.40177**

## INTRODUCTION

High-performance aromatic polyimides (PIs) possess various outstanding properties, such as high thermal, mechanical, and chemical resistance and a low dielectric constant. Therefore, increasing attention has been paid to the application of PIs to microelectronics, optoelectronics, and the aerospace industry.[1,2] However, they have a few limitations, such as low electrical conductivity, electrostatic accumulation, and poor heat dissipation. These limitations must be resolved before aromatic polyimides can be used for special applications. One way to resolve these issues is by incorporating carbon nanofillers, which can effectively enhance the thermal, mechanical, and electrical properties of the nanocomposites.[3,4]

Although carbon nanofillers such as carbon nanotubes and carbon black are effective in improving the mechanical and electrical properties of PI, they are very difficult to disperse in organic solvents that have a high content of carbon nanofillers due to van der Waals force.[5,6] A planar sheet of graphene has a single-atom thickness and is made up of $sp^2$-bonded carbon atoms that are densely packed in a honeycomb crystal lattice.[7] This structure has led to a wide interest in graphene in the fields of nanoscience and condensed matter physics because of its exceptional electrical,[8] physical,[9] and chemical properties.[10] Excellent properties such as extraordinary electronic transport capabilities, mechanical performance, high surface area, and distinctive mechanical properties with fracture strains of ~25% and a Young's modulus of ~1 TPa have opened new pathways for the development of a wide range of new functional materials. However, poor dispersion in organic solvents limits the widespread use of graphene. In contrast, graphene oxide (GO), which is produced through the chemical oxidation of graphite, disperses effectively in polar solvents due to functional groups such as ketones, diols, epoxides, hydroxyls, and carbonyl. Recently, many researchers have developed reduced-graphene oxide (r-GO)/PI nanocomposites to improve the mechanical and electrical properties of composite materials via in situ polymerization with a small amount of GO (<10 wt %).[2,11] However, few reports have focused on nanocomposites with a high content of GO.

In this study, we outline an effective method for preparing r-GO/PI composite materials via in situ polymerization with a GO content of up to 30% for high performance nanocomposites. Electrical, thermal, and mechanical properties of the resulting r-GO/PI composite films were performed and scanning electron microscopy was used to oberve morphology of fractued surface of films. We also investigated the effect of homogeneouly dispersed r-GO in PI on the oxygen transmission rate.

## EXPERIMENTAL

### Chemicals

4,4′-oxydianiline (ODA, 99%), pyromellitic dianhydride (PMDA, 99%), *N*-Methy1–2-pyrrolidone (NMP, 99.5%) and potassium permanganate ($KMnO_4$, 99.0%) obtained from Sigma-Aldrich were used. High purity graphite flakes (325 mesh, 98%) were purchased from Johnson Matthey Sulfuric acid ($H_2SO_4$, 97%) and hydrogen peroxide ($H_2O_2$, 30 wt %) were supplied by Matsunoen Chemicals and Daejung Chemical & Metals, respectively.

### Synthesis of Graphene Oxide

A modified Hummers Method was used to obtain graphene oxide (GO) for the purposes of this study.[12] Graphite flakes (4 g) were added to a 250-mL round-bottomed flask containing concentrated $H_2SO_4$ (120 mL) and stirred for 1 h. Nine portions of 15 g $KMnO_4$ were then added at 20-min intervals while stirring. The temperature was slowly increased to 40°C and maintained for 5 h in order to fully oxidize the graphite. Subsequently, 150 mL of deionized (DI) water was added to the solution. A 15 mL $H_2O_2$ solution was added to the mixture over a 30-min interval while stirring and the mixture was left for 24 h. After centrifuging, the mixture in the dialysis tube was washed with DI water several times to obtain a pH of 5. Finally, a freeze dryer was used at −45°C for 24 h to remove residue in the GO.

### Synthesis of Polyamic Acid (PAA) and Its Composite Solutions

Three portions of PMDA (1 g, 4.6 mmol) were added to a solution of ODA (0.918 g, 4.6 mmol) in NMP (10 mL). An additional NMP solution was added until the solid content was adjusted to 15% by weight. The mixture was stirred at room temperature for 24 h to produce a viscous and homogeneous PAA. Taking the 1 wt % GO/PAA composite solution as an example, the detailed synthesis procedures were as follows: 0.019 g of GO obtained from a modified Hummers Method was added to a certain amount of NMP, and the mixture was subjected to ultrasonic waves for 2 h. The GO was completely exfoliated to achieve a uniform dispersion in this process. Then, 0.918 g of ODA was added to the GO solution while stirring for 30 min. Subsequently, 1 g of PMDA divided into three portions was added to the mixture at 30-min intervals and maintained the mixture while stirring for 24 h after adding the final portion of PMDA. Finally, a 1 wt % GO/PAA solution was obtained with the desired viscosity. A series of GO/PAA composite solutions with different GO loadings (1∼30 wt %) were prepared in the same way.

### Preparation of Pure PI and Its Composite Films

The conventional solvent casting method was performed to make the PAA and GO/PAA composite films. A horizontal bar was used to control the thicknesses of the films with a casting speed of 6 mm $s^{-1}$. Pure PAA and GO/PAA solutions with a thickness of ∼750 μm were cast onto the commercial PI film. All the cast films were dried at 90°C for 2 h in a vacuum oven to remove the residual solvent and then thermally imidized under a nitrogen atmosphere with a temperature increase of 3°C $min^{-1}$. The heating process is shown in Figure 1. All the films were allowed to cool to 25°C once they had achieved a maximum temperature of 400°C for 30 min. The final thicknesses of films were found to be ∼50 μm. The entire process is displayed in Figure 2.

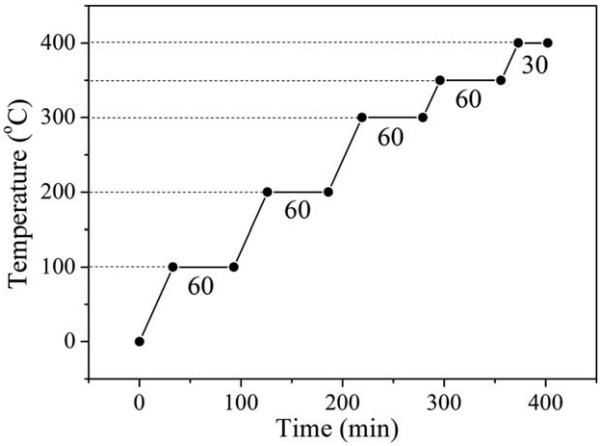


**Figure 1.** The procedures of imidization of pure PI and its composite films.

### Characterization

The chemical reaction was confirmed by Fourier transform-infrared spectroscopy (FTIR Spectrophotometer, Nicolet IS10, USA). Each sample was scanned 16 times at a resolution of 16 $cm^{-1}$ with a range of 400∼4000 $cm^{-1}$. Electrical conductivities were measured using a four probe resistivity meter (FPP-RS8, Dasol Eng., Korea) and a super megohmmeter (SM-8200, Hioki, Japan). Thermogravimetric analysis (TGA) was performed in order to investigate the stability of pure PI and r-GO/PI composites in a nitrogen atmosphere at a temperature increase of 10°C/min using a TGA Q50 (TA Instruments, USA). Tensile property was tested using an Instron Universal Tester 5567 (Instron, USA) with a crosshead speed of 5 mm $min^{-1}$. The length and width of the specimen were 3.0 and 0.5 cm, respectively. Specimens were loaded on a paper tab with a 2.5 cm gauge length. For enhancing the gripping, an epoxy resin was applied to both ends of specimens, and cured for 24 h at 50°C. At least 10 specimens were prepared for each test. Young's Modulus, $E$, was defined as the ratio of the stress along an axis over the strain along that axis in the initial portion of the stress-strain curve. Therefore, it can be calculated by using the following equation;

$$E = \text{tensile stress}/\text{tensile strain} = (F/A_0)/(\Delta L/L_0)$$

where, $E$ is the Young's modulus, $F$ is the force exerted on an object under tension, $A_0$ is the original cross-sectional area through which the force is applied, $\Delta L$ is the amount by which

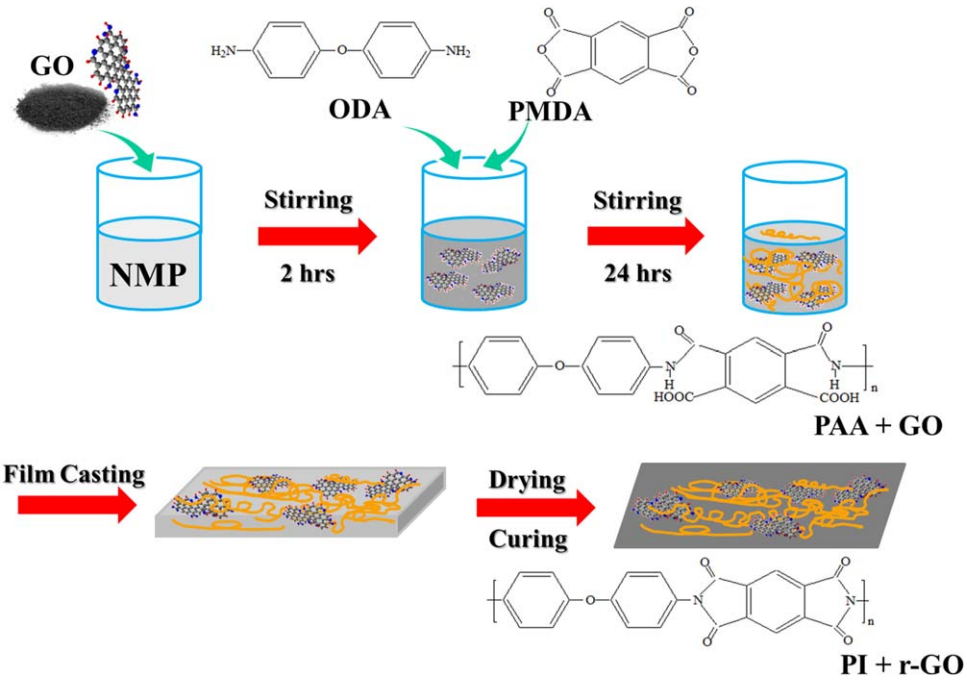


**Figure 2.** The procedures of the synthesis of pure PI and its composite films. [Color figure can be viewed in the online issue, which is available at wileyonlinelibrary.com.]

the length of the object changes, $L_0$ is the original of the object.[13]

Composite samples were embedded in epoxy resin and ultramicrotomed for morphological study. Transmission electron microscope (TEM, FEI Tecnai G2 F20, USA) was used for investigating morphology of GO in composite forms containing 5, 10, and 20 wt % GOs. After microtoming at 25°C, samples were dispensed on a carbon grid. Field emission scanning electron microscopy (FE-SEM, HITACHI S-4700, Japan) was performed at an acceleration voltage of 15 kV to observe the morphology of the fractured surfaces with regards to pure PI and its composites after tensile testing. The oxygen transmission rates (OTRs) of PI and its composite films were measured based on continuous pressure applied by a film permeability testing machine (OX-TRAN Model 2/21, MOCON, USA) at 25°C according to ASTM D 3985.

## RESULTS AND DISCUSSION

### Synthesis and Characterization of Pure PI and Its Composites

FTIR was employed to confirm the conversion of PAA to PI and the spectra of all the samples are shown in Figure 3. In Figure 3(a), absorption peaks of 1640 and 1538 $cm^{-1}$ were ascribed to carbonyl in CONH stretching bands and C—NH stretching, respectively.[14,15] The peak at 1714 $cm^{-1}$ was attributed to C=O in the COOH group in the PAA macromolecules.[2] As shown in Figure 3(b), two peaks at 1774 and 1714 $cm^{-1}$ can be explained by C=O asymmetric stretching and C=O symmetric stretching of imide. Moreover, the disappearance of absorption peaks at 1640 and 1538 $cm^{-1}$ and the evident new absorption bands at 1367 and 721 $cm^{-1}$ in the FTIR spectrum of pure PI, which were ascribed to C—N stretching and C=O bending of imide, respectively, were observed. This indicates the presence of an imide group and the completion of imidization.[16–18] However, there was no significant difference observed between pure PI and r-GO/PI composites, which also showed characteristic absorptions of the imide unit at 1774, 1714, 1367, and 721 $cm^{-1}$. The FTIR results demonstrated the successful synthesis of PI and r-GO/PI composite films in this experiment.

### Electrical Conductivity

An ultra megohmmeter and a four-probe unit were performed to measure the electrical conductivities of pure PI and r-GO/PI composite films. As shown in Figure 4, the electrical conductivity of each sample increased as the loading of GO increased. As summarized in Table I, the electrical conductivity of the r-GO/PI composite containing 20 wt % of GO was found to be $8.9 \times 10^{-1}$ S $m^{-1}$, an increase of more than twelve orders of magnitude compared with pure PI ($1.66 \times 10^{-13}$ S $m^{-1}$). This was due to the electrical percolation networks of the partially reduced GO in the composite.[19] Nevertheless, the electrical conductivity only increased to $1.1 \times 10^{1}$ S $m^{-1}$ as GO loading was increased to 30 wt %, owing to the saturation of r-GO in composites transferred from the GO during the chemical imdization process. The evolution of electrical conductivity with increasing GO loading can be described using the power law[20];

$$\sigma \propto \mu(v - v_c)^t$$

where $\sigma$, $v$, and $t$ are the electrical conductivity, volume fraction of GO, and the critical exponent, respectively, and the subscript $c$ represents critical value at the percolation threshold. Based on the electrical conductivity evolution illustrated in Figure 4, the critical exponent, $t$, is calculated to be 3.7. In Figure 5, TEM micrographs indicated GO networks of composites containing 20 wt % GO compared with 5 or 10 wt % GO composites. Interestingly, various shapes of GO aggregates were observed,

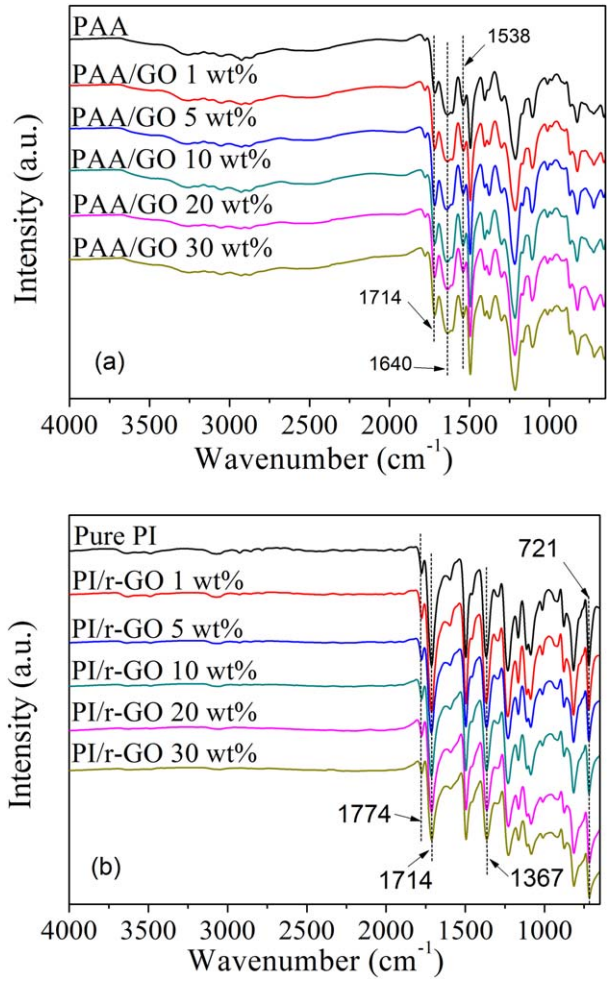


**Figure 3.** FTIR spectra of (a) pure PAA and its composites, (b) pure PI and its composites with various GO loadings. [Color figure can be viewed in the online issue, which is available at wileyonlinelibrary.com.]

which may lead to relatively higher the critical exponent than those in other GO composites due to multiple percolation.[21,22]

### Thermal Analysis

Thermal properties are very important for PI and its composite films when they are used as high performance heat-resistant engineering plastics. Therefore, TGA was performed to characterize the thermal stability of the PI and r-GO/PI composites in a nitrogen atmosphere at a temperature increase of 10°C $min^{-1}$. The thermal stability of the composite films slightly

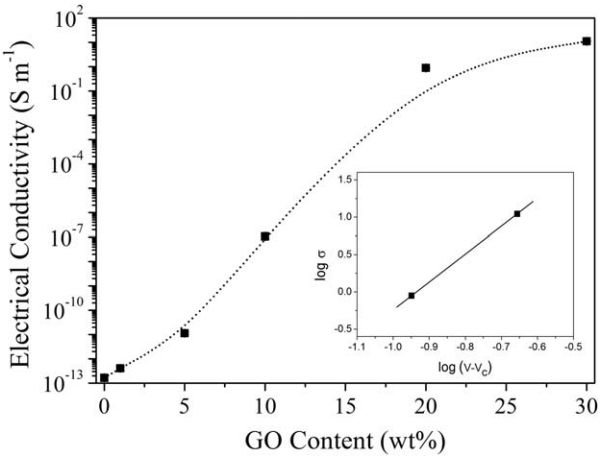


**Figure 4.** The electrical conductivities of pure PI and r-GO/PI with various loadings of GO.

decreased with the increase of GO loading. This is because the functional groups such as ketones, diols, and epoxides still remain in graphene even after thermal imidization. As shown in Figure 6, the weight loss of all the samples that occurred at the beginning was due to the evaporation of stored water.[23–26] Major weight loss of r-GO/PI containing 1 wt % GO was detected until the temperature was increased to around 570°C, similar to that of pure PI film. It reached ~450°C as the GO loading increased to 30 wt %. This was due to pyrolysis of the labile oxygen functional groups of the GO that remained in the composites after chemical imidization.[1] All samples displayed excellent thermal stability at elevated temperature (>400°C). Therefore, the results indicated that pure PI and its composite films possess a thermal stability that is able to withstand harsh environments and can be used for high-tech applications.

### Mechanical Properties

Figure 7 shows the representative stress–strain curves of pure PI and its composite films and the tensile properties are summarized in Table I. It is widely believed that external stress on a plastic composite is transferred from the continuous phase (polymer maxtrix) to the discontinuous phase (filler) and that the final properties depend on the extent of the bonding between the two phases.[1] Therefore, tensile stress decreased from 127.7 MPa of pure PI to 70.0 MPa of r-GO/PI containing 30 wt % GO due to the addition of fillers in the composite, resulting in the phase separation of r-GO from the PI matrix.[27] However, the corresponding Young's modulus significantly

**Table I.** Electrical and Mechanical Properties of Pure PI and Its Composites

| Sample | Conductivity (S $m^{-1}$) | Young's modulus (GPa) | Tensile strength (MPa) | Elongation at break (%) |
|---|---|---|---|---|
| Pure PI | $(1.66 \pm 0.45) \times 10^{-13}$ | $1.1 \pm 0.0$ | $127.7 \pm 4.2$ | $52.0 \pm 7.3$ |
| r-GO/PI (1 wt %) | $(4.10 \pm 0.78) \times 10^{-13}$ | $1.5 \pm 0.2$ | $115.3 \pm 3.9$ | $38.6 \pm 4.7$ |
| r-GO/PI (5 wt %) | $(1.13 \pm 0.12) \times 10^{-12}$ | $1.9 \pm 0.2$ | $107.2 \pm 3.9$ | $22.4 \pm 2.7$ |
| r-GO/PI (10 wt %) | $(1.07 \pm 0.20) \times 10^{-7}$ | $2.7 \pm 0.1$ | $106.8 \pm 2.7$ | $12.5 \pm 1.0$ |
| r-GO/PI (20 wt %) | $(8.91 \pm 0.34) \times 10^{-1}$ | $3.1 \pm 0.1$ | $84.7 \pm 5.0$ | $5.6 \pm 0.6$ |
| r-GO/PI (30 wt %) | $(1.10 \pm 0.04) \times 10^{1}$ | $4.2 \pm 0.1$ | $70.0 \pm 6.7$ | $2.2 \pm 0.3$ |

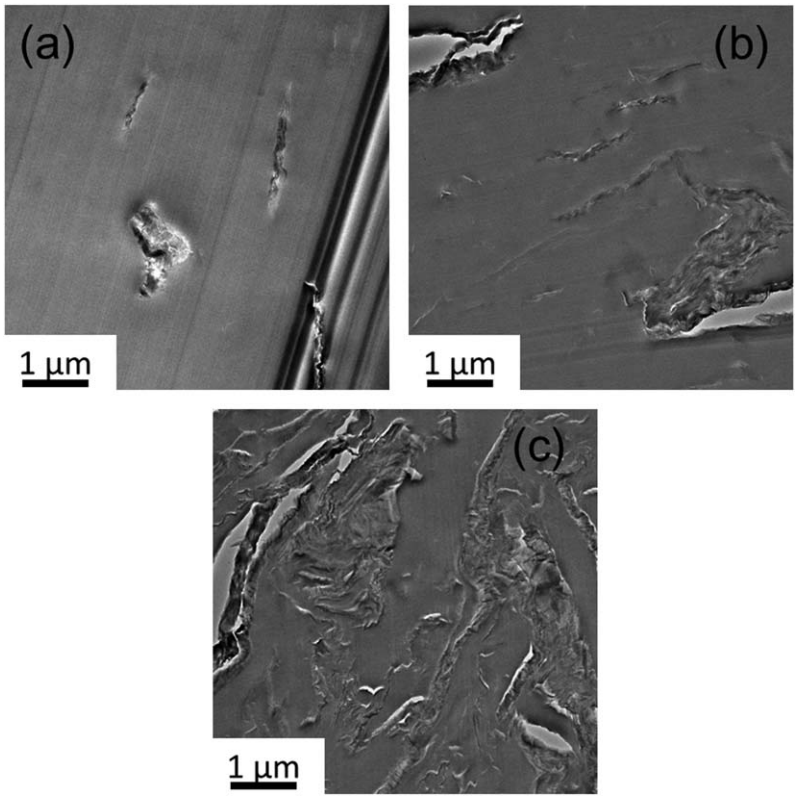


**Figure 5.** TEM micrographs of the microtomed compsoites containing (a) 5, (b) 10, and (c) 20 wt% GO.

increased by 282% from 1.1 GPa to 4.2 GPa owing to the non-covalent and molecular-level interaction between the r-GO and PI matrix.[28] In addition, tensile elongation decreased significantly when even only 1 wt % GO was added to the polymer. This was likely due to small agglomerates, produced by the excess GO and acting as stress concentration sites, thus becoming one of the possible origins of the embrittlement of the composites.[29] To better understand the mechanical properties of r-GO/PI composites, SEM was used to observe the fractured surface images of all samples after tensile testing. As shown in Figure 8, the fractured surface of r-GO/PI composite was relatively rough compared to that of pure PI. In addition, it was clearly observed that the GO was dispersed throughout the PI films.

### Barrier Properties

The oxygen barrier property of each film was determined by using a commercial MOCON instrument. The OTRs of pure PI and r-GO/PI composite films measured at 25°C were shown in Figure 9, and the trend line is plotted using Sigmoidal-

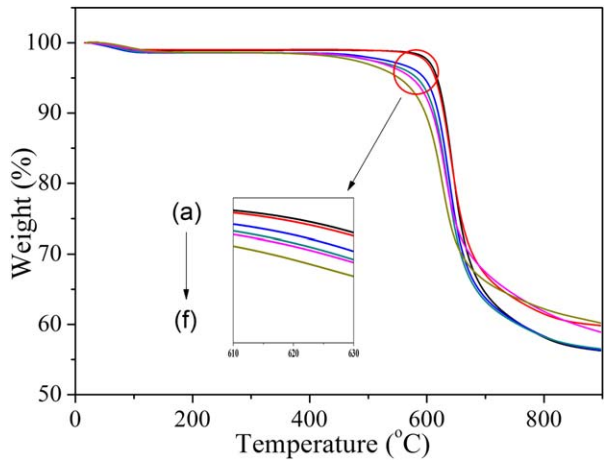


**Figure 6.** TGA thermograms of pure PI and its composite films containing various amounts of GO: (a) pure PI, (b) 1, (c) 5, (d) 10, (e) 20, and (f) 30 wt %. [Color figure can be viewed in the online issue, which is available at wileyonlinelibrary.com.]

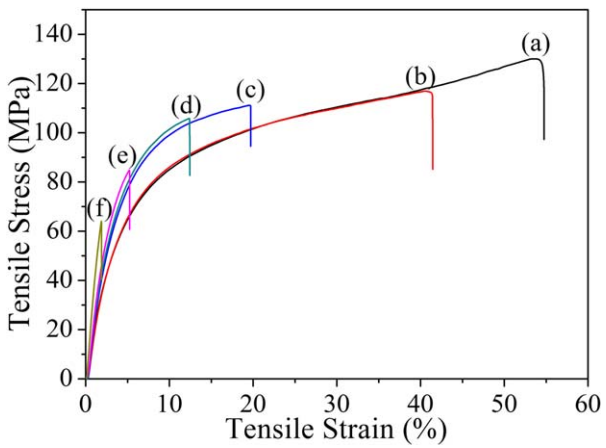


**Figure 7.** Stress–strain curves of pure PI and its composites with various GO loadings: (a) pure PI, (b) 1, (c) 5, (d) 10, (e) 20, and (f) 30 wt %, respectively. [Color figure can be viewed in the online issue, which is available at wileyonlinelibrary.com.]

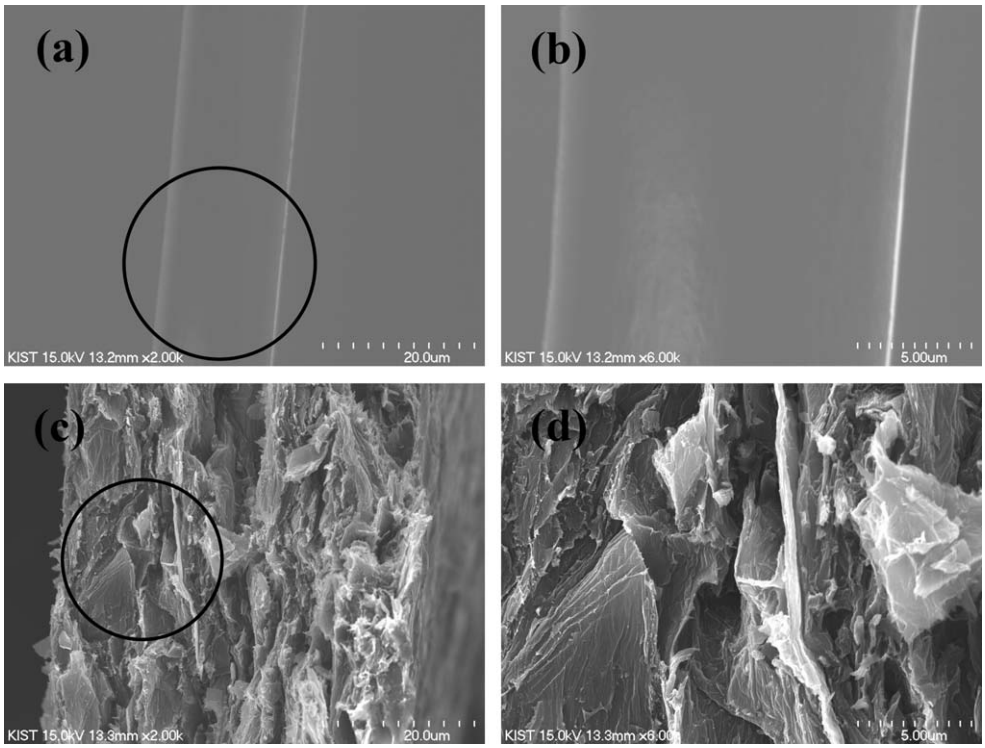


**Figure 8.** SEM micrographs of the fractured surface of pure PI (a,b) and 30 wt % r-GO/PI (c,d) with various magnifications.

Boltzman eqaution. As expected, the OTR of the r-GO/PI composite decreased continuously with increased GO loading. It decreased significantly from 377.78 of pure PI to 26.07 $cm^3$ $m^{-2}$ 24 $h^{-1}$ $atm^{-1}$ of the 30 wt % GO loading composite, which displayed a 93% reduction compared with pure PI. This could be determined by the molecular-level dispersion of the r-GO with a high aspect ratio and high specific surface area in the PI matrix, resulting in a convoluted dispersion path and a reduced cross-section for oxygen diffusion.[27,30–32] Moreover, hydrogen bonding of the permeating oxygen molecules and the hydroxyl groups could occur along the edges of the GO remaining in the PI matrix after heat treatment, also contributing to reduced permeability.[33] Furthermore, it is noted that a dramatic decrease was observed with composites containing 20 wt % GO, and a similar result was found in a volume resistivity measurement, indicating that GO networks help not only to create conductive pathways but also to prevent oxygen diffusion. The results demonstrated that r-GO/PI composite films could be potentially used as a packaging material for protecting goods against oxygen degradation.

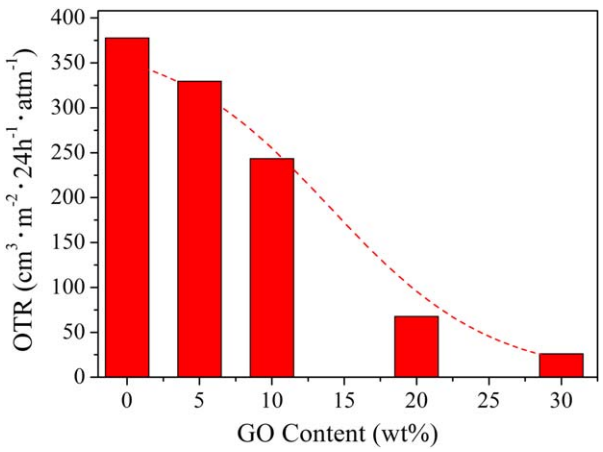


**Figure 9.** The OTRs of pure PI and r-GO/PI with various loadings of GO. [Color figure can be viewed in the online issue, which is available at wileyonlinelibrary.com.]

## CONCLUSIONS

In summary, we prepared graphene oxide (GO) using a modified Hummers method. r-GO/PI composites were prepared by in situ polycondensation of aromatic dianhydride and aromatic diamine with GO via soluble polyamic acid, followed by thermal curing at an elevated temperature. The r-GO/PI composites showed a 282% increase in Young's modulus containing with the hightest GO content (~30 wt %). Furthermore, the oxygen transmission rate (OTR) of the r-GO/PI composites was also significantly reduced due of the molecular-level dispersion of the r-GO and the electrical conductivity of the PI composites containing 30 wt % GO increased 14-fold compared with pure PI. These results indicate that highly exfoliated GO with a high thermal treatment at 400°C would be a simple and effective way to develop multifunctional nanocomposites for a wide range of applications.

## ACKNOWLEDGMENTS

This study was supported by the Korea Institute of Science and Technology (KIST) Institutional Program, and supported by a

grant from by the Ministry of Trade, Industry and Energy of Korea (2MR0760).

## REFERENCES


1. Kim, G. Y.; Choi, M.-C.; Lee, D.; Ha, C.-S. *Macromol. Mater. Eng.* **2012**, *297*, 303.
2. Luong, N. D.; Hippi, U.; Korhonen, J. T.; Soininen, A. J.; Ruokolainen, J.; Johansson, L.-S.; Nam, J.-D.; Sinh, L. H.; Seppälä, J. *Polymer* **2011**, *52*, 5237.
3. Jiang, X. W.; Bin, Y. Z.; Matsuo, M. *Polymer* **2005**, *46*, 7418.
4. Ounaies, Z.; Park, C.; Wise, K. E.; Siochi, E. J.; Harrison, J. S. *Compos. Sci. Technol.* **2003**, *63*, 1637.
5. Verdejo, R.; Mar Bernal, M.; Romasanta, L. J., Lopez-Manchado, M. A. *J. Mater. Chem.* **2011**, *21*, 3301.
6. Vaia, R. A.; Daniel Wagner, H. *Materialstoday* **2004**, *7*, 32.
7. Rao, C. N. R.; Sood, A. K.; Subrahmanyam, K. S.; Govindaraj, A. *Angew Chem Int Ed.* **2009**, *48*, 7752.
8. Lee, C.; Wei, X. D.; Kysar, J. W.; Hone, J. *Science* **2008**, *321*, 385.
9. Balandin, A. A. *Nat. Mater.* **2011**, *10*, 569.
10. Dutta, S.; Pati, S. K. *J. Mater. Chem.* **2010**, *20*, 8207.
11. Park, O. K.; Hwang, J.-Y.; Go, M. J.; Lee, J. H.; Ku, B-C.; You, N-H. *Macromolecules* **2013**, *46*, 3505.
12. Hummers, W. S.; Offeman, R.E. *J. Am. Chem. Soc.* **1985**, *80*, 1339.
13. IUPAC. Compendium of Chemical Terminology, 2nd ed., **1997**, p 12.
14. Zhang, Q.; Wu, D. Z.; Qi, S.; Wu, Z. P.; Yang, X. P.; Jin, R. G. *Mater. Lett.* **2007**, *61*, 4027.
15. Zheng, Z. X.; Wang, Z. H.; Feng, Q. L.; Zhang, F. Y.; Du, Y. L.; Wang, C. M. *Mater. Chem. Phys.* **2013**, *138*, 350.
16. Tang, Q. Y.; Chen, J.; Chan, Y. C.; Chung, C. Y. *Polym. Degrad. Stabil.* **2010**, *95*, 1672.
17. Boroglu, M. S.; Boz, I.; Gurkaynak M. A. *Polym. Adv. Technol.* **2006**, *17*, 6.
18. Chu, H. J.; Zhu, B. K.; Xu, Y. Y. *Polym. Adv. Technol.* **2006**, *17*, 366.
19. Rahaman, M.; Chaki, T.K.; Khastgir, D. *J. Mater. Sci.* **2011**, *46*, 3989.
20. Rahaman, M.; Chaki, T. K.; *Khastgir. Compos. Sci. Technol.* **2012**, *72*, 1575.
21. He, L.; Tjong, S. C. *Nanoscale Res. Lett.* **2013**, *8*, 132.
22. Leyva, M. E.; Barra, G. M. O.; Moreira, A. C. F.; Soares, B. G.; Khastgir, D. *J. Polym. Sci. Polym. Phys.* **2003**, *41*, 2983.
23. Bao, H. Q.; Pan, Y. Z.; Ping, Y.; Sahoo, N. G.; Wu, T. F.; Li, L.; Li, J.; Gan, L. H. *Small* **2011**, *11*, 1569.
24. Jung, I.; Dikin, D.; Park, S.; Cai, W. W.; Mielke, S. L.; Ruoff, R. S. *J. Phys. Chem. C*, **2008**, *112*, 20264.
25. Schniepp, H. C.; Li, J. L.; McAllister, M. J.; Sai, H.; Herrera-Alonsom, M.; Adamson, D. H.; Prud'homme, R. K.; Car, R.; Saville, D. A.; Aksay, I. A. *J. Phys. Chem. B* **2006**, *110*, 8535.
26. Shen, J. F.; Hu, Y. Z.; Li, C.; Qin, C.; Shi, M.; Ye, M. X. *Langmuir* **2009**, *25*, 6122.
27. Wu, J. R.; Huang, G. S.; Li, H.; Wu, S. D.; Liu, Y. F.; *Zheng. Polymer* **2013**, *54*, 1930.
28. Al-Kandary, S. H.; Ali, A. A. M.; Ahmad, Z. *J. Mater. Sci.* **2006**, *41*, 2907.
29. Chen, D.; Zhu, H.; Liu, T. X. *ACS Appl. Mater. Inter.* **2010**, *2*, 3702.
30. Tsai, M.-H.; Chang, C.-J.; Lu, H.-H.; Liao, Y.-F.; Tseng, I.-H. *Thin Solid Films*, **2013**, http://dx.doi.org/10.1016/j.tsf.2013.02.105.
31. Compton, O. C.; Kim, S.; Pierre, C.; Torkelson, J. M.; Nguyen, S. T. *Adv. Mater.* **2010**, *22*, 4759.
32. Yang, Y. H.; Bolling, L.; Priolo, M. A.; Grunlan, J. C. *Adv. Mater.* **2013**, *25*, 503.
33. Huang, H. D.; Ren, P. G.; Chen, J.; Zhang, W. Q.; Ji, X.; Li, Z. M. *J. Membr. Sci.* **2012**, *156*, 409.